

University of Groningen

## Exogenous Ligand-Free Nickel-Catalyzed Carboxylate O-Arylation

Wolzak, Lukas A.; de Zwart, Felix J.; Oudsen, Jean Pierre H.; Bartlett, Stuart A.; de Bruin, Bas; Reek, Joost N.H.; Tromp, Moniek; Korstanje, Ties J.

*Published in:*  
 ChemCatChem

*DOI:*  
[10.1002/cctc.202200547](https://doi.org/10.1002/cctc.202200547)

**IMPORTANT NOTE:** You are advised to consult the publisher's version (publisher's PDF) if you wish to cite from it. Please check the document version below.

*Document Version*  
 Publisher's PDF, also known as Version of record

*Publication date:*  
 2022

[Link to publication in University of Groningen/UMCG research database](#)

*Citation for published version (APA):*

Wolzak, L. A., de Zwart, F. J., Oudsen, J. P. H., Bartlett, S. A., de Bruin, B., Reek, J. N. H., Tromp, M., & Korstanje, T. J. (2022). Exogenous Ligand-Free Nickel-Catalyzed Carboxylate O-Arylation: Insight into Ni/Ni<sup>III</sup> Cycles\*\*. *ChemCatChem*, 14(18), [e202200547]. <https://doi.org/10.1002/cctc.202200547>

### Copyright

Other than for strictly personal use, it is not permitted to download or to forward/distribute the text or part of it without the consent of the author(s) and/or copyright holder(s), unless the work is under an open content license (like Creative Commons).

The publication may also be distributed here under the terms of Article 25fa of the Dutch Copyright Act, indicated by the "Taverne" license. More information can be found on the University of Groningen website: <https://www.rug.nl/library/open-access/self-archiving-pure/taverne-amendment>.

### Take-down policy

If you believe that this document breaches copyright please contact us providing details, and we will remove access to the work immediately and investigate your claim.

*Downloaded from the University of Groningen/UMCG research database (Pure): <http://www.rug.nl/research/portal>. For technical reasons the number of authors shown on this cover page is limited to 10 maximum.*

WILEY-VCH

 **Chemistry  
Europe**

European Chemical  
Societies Publishing

# Take Advantage and Publish Open Access



By publishing your paper open access, you'll be making it immediately freely available to anyone everywhere in the world.

That's maximum access and visibility worldwide with the same rigor of peer review you would expect from any high-quality journal.

**Submit your paper today.**



[www.chemistry-europe.org](http://www.chemistry-europe.org)



# Exogenous Ligand-Free Nickel-Catalyzed Carboxylate *O*-Arylation: Insight into Ni<sup>I</sup>/Ni<sup>III</sup> Cycles\*\*

Lukas A. Wolzak,<sup>[a, b]</sup> Felix J. de Zwart,<sup>[b]</sup> Jean-Pierre H. Oudsen,<sup>[c]</sup> Stuart A. Bartlett,<sup>[d]</sup> Bas de Bruin,<sup>[b]</sup> Joost N. H. Reek,<sup>\*,[b]</sup> Moniek Tromp,<sup>\*,[a, e]</sup> and Ties J. Korstanje<sup>\*,[a]</sup>

Nickel-catalyzed cross-coupling reactions have become a powerful methodology to construct C–heteroatom bonds. However, many protocols suffer from competitive off-cycle reaction pathways and require non-equimolar amounts of coupling partners to suppress them. Here, we report on mechanistic examination of carboxylate *O*-arylation under thermal conditions, in both the presence and absence of an exogenous bipyridine-ligand. Furthermore, spectroscopic studies of the novel ligand-free carboxylate *O*-arylation reaction

unveiled the resting state of the nickel catalyst, the crucial role of the alkylamine base and the formation of an off-cycle Ni<sup>I</sup>–Ni<sup>II</sup> dimer upon reduction. This study provides insights into the competition between productive catalysis and deleterious pathways (comproportionation and protodehalogenation) in the commonly proposed self-sustained Ni<sup>I</sup>/Ni<sup>III</sup> catalytic cycle. Thereby we show that for productive nickel-catalyzed carboxylate *O*-arylation a choice must be made between either mild conditions or equimolar ratios of substrates.

## Introduction

In recent years, nickel catalysis has enabled the formation of challenging C–heteroatom bonds, resulting in previously elusive cross-coupling reactions that can now be performed under mild conditions.<sup>[1–3]</sup>

An example hereof is the coupling of carboxylic acids and aryl halides to form *O*-aryl esters enabled by (dtbbpy)NiX<sub>2</sub> under photochemical,<sup>[4–8]</sup> electrochemical<sup>[9]</sup> or thermal reaction conditions<sup>[10]</sup> (Figure 1A). This cross-coupling reaction is notably demanding due to the low nucleophilicity of the carboxylate group. Although analogous *O*-aryl ester bond formation reactions catalyzed by palladium have been reported, these protocols are far from mild and efficient, and are relying on stoichiometric amounts of silver salts.<sup>[11,12]</sup> Mechanistically, nickel-catalyzed C–heteroatom bond formations under thermal conditions were proposed to proceed via a self-sustained Ni<sup>I</sup>/Ni<sup>III</sup> catalytic cycle.<sup>[10]</sup> In addition, the relevance of this catalytic mechanism was also demonstrated under photochemical<sup>[13–17]</sup> and electrochemical<sup>[14]</sup> reaction conditions.

From these catalytic studies it became apparent that in order to successfully engage a self-sustained Ni<sup>I</sup>/Ni<sup>III</sup> catalytic cycle the continuous reduction of Ni<sup>II</sup> to Ni<sup>I</sup> is required, as Ni<sup>I</sup> is prone to deactivation via an exergonic comproportionation reaction with Ni<sup>III</sup> forming inactive Ni<sup>II</sup>. Besides catalytic studies, another important approach to elucidate catalytic pathways has been provided by the synthesis, characterization and *in situ* generation of Ni<sup>I</sup> complexes and the study of their reactivity. Investigations have unveiled that specific Ni<sup>I</sup>-complexes bearing a bipyridine (bpy) based ligand<sup>[14,18–20]</sup> are indeed able to activate aryl halides<sup>[14,19]</sup> and that the required Ni<sup>III</sup> state can be accessed via oxidative addition of a Ni<sup>I</sup> complex.<sup>[21,22]</sup> So far mechanistic insights through catalytic studies and stoichiometric reactions have demonstrated the validity of the elementary steps proposed in the self-sustained Ni<sup>I</sup>/Ni<sup>III</sup> catalytic cycle. However, these catalytic and stoichiometric studies do not

[a] L. A. Wolzak, Prof. M. Tromp, Dr. T. J. Korstanje  
Sustainable Materials Characterization, van 't Hoff Institute for Molecular Sciences (HIMS)  
University of Amsterdam  
Science Park 904  
1098 XH Amsterdam (The Netherlands)  
E-mail: t.j.korstanje@uva.nl  
moniek.tromp@rug.nl

[b] L. A. Wolzak, F. J. de Zwart, Prof. B. de Bruin, Prof. J. N. H. Reek  
Bio-inspired, Homogeneous and Supramolecular Catalysis, van 't Hoff Institute for Molecular Sciences (HIMS)  
University of Amsterdam  
Science Park 904  
1098 XH Amsterdam (The Netherlands)  
E-mail: j.n.h.reek@uva.nl

[c] Dr. J.-P. H. Oudsen  
Metalloenzyme Group  
Department of Physical / Biophysical Chemistry  
Technical University Berlin  
Straße des 17. Juni 135  
10623 Berlin (Germany)

[d] Dr. S. A. Bartlett  
Diamond Light source (DLS)  
Harwell Science and Innovation Campus  
Didcot, Oxfordshire OX11 0DE (UK)

[e] Prof. M. Tromp  
Faculty of Science and Engineering, Materials Chemistry  
Zernike Institute for Advanced Materials  
University of Groningen  
Nijenborgh 4  
9747 AG Groningen (The Netherlands)

[\*\*] A previous version of this manuscript has been deposited on a preprint server (<https://doi.org/10.26434/chemrxiv-2022-k12lw>)

Supporting information for this article is available on the WWW under <https://doi.org/10.1002/cctc.202200547>

This publication is part of a joint Special Collection with EurJOC and EurJIC on the Netherlands Institute for Catalysis Research. Please see our homepage for more articles in the collection.

© 2022 The Authors. ChemCatChem published by Wiley-VCH GmbH. This is an open access article under the terms of the Creative Commons Attribution Non-Commercial License, which permits use, distribution and reproduction in any medium, provided the original work is properly cited and is not used for commercial purposes.

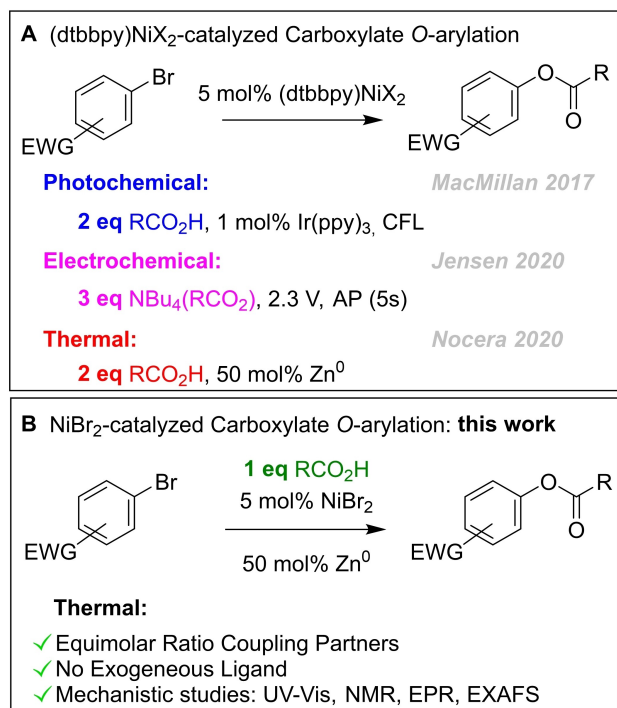


**Figure 1.** Nickel Catalyzed Cross-Coupling between aryl halides and carboxylic acids using A) (dtbbpy)NiX<sub>2</sub> system or B) Ligand-Free system. (dtbbpy = 4,4'-di-tert-butyl-2,2'-bipyridine, AP = alternating polarity).

account for the non-equimolar ratios of substrates often required for productive C–heteroatom bond formations. Therefore, to further develop the field of nickel cross-coupling and enable more efficient reactions, a better understanding of the competition between fundamental elementary steps and off-cycle reaction pathways is required.

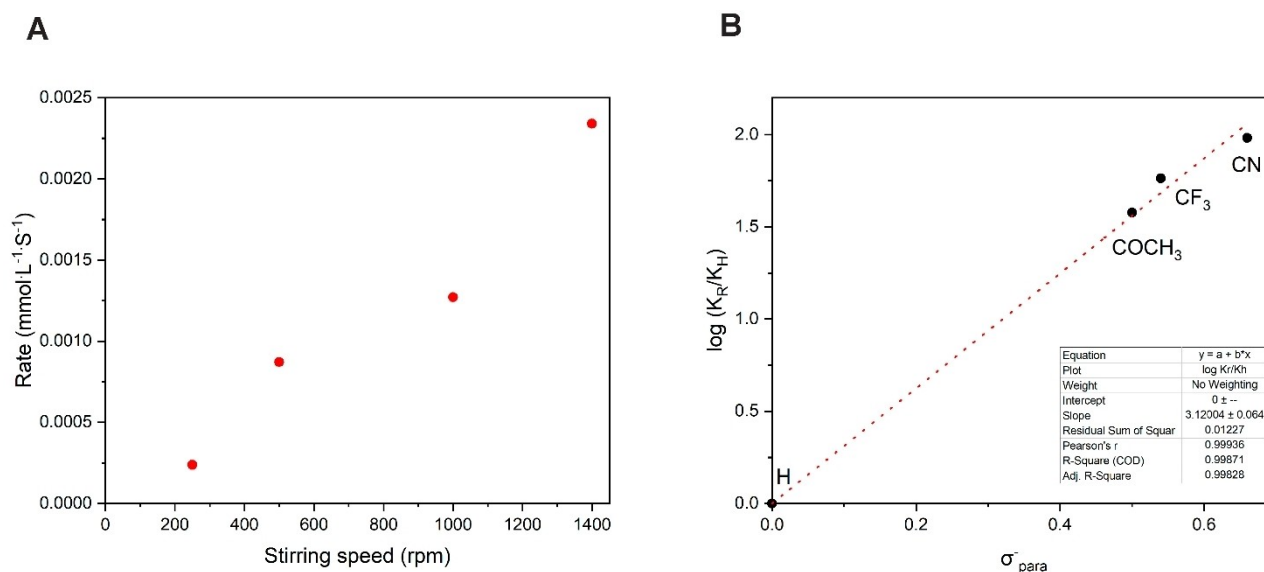
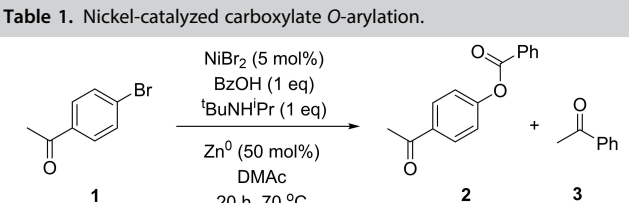


**Figure 2.** Kinetic investigations on the nickel system. [A] Rate dependency on the stirring speed of the NiBr<sub>2</sub>-catalyzed reaction of 4-bromoacetophenone and benzoic acid. [B] Hammett plot for NiBr<sub>2</sub>-catalyzed esterification of bromobenzene derivatives with benzoic acid.

**Table 1.** Nickel-catalyzed carboxylate O-arylation.



Entry <sup>[a]</sup>	Deviation	Conv. 1 [%]	Yield 2 [%]	Yield 3 [%]
1	–	100	81	9
2	In dark	100	76	13
3	2 eq BzOH and 2 eq <sup>t</sup> BuNH <sup>t</sup> Pr	100	89	6
4	5 mol% dtbbpy	100	61	38
5	40 °C	15	12	2
6	Ni(OBz) <sub>2</sub>	100	83	15
7	DMF as solvent	21	19	2
8	Bu <sub>4</sub> N(OBz) as substrate	21	7	5
9	2 eq <sup>t</sup> BuNH <sup>t</sup> Pr	100	90	10

[a] Conditions: Bromoacetophenone (200 mM) Benzoic Acid (200 mM), <sup>t</sup>BuNH<sup>t</sup>Pr (200 mM) Nickel(II) bromide (5 mol%), Zinc (50 mol%), DMAc (6 mL), 20 hours, 70 °C. [a] Determined by GC analysis.

## Results and Discussion

**Approach.** Exogenous Ligand-free protocols have been reported for nickel-catalyzed C–N cross-coupling reactions,<sup>[23,24]</sup> and therefore a similar approach to carboxylate O-arylation could be feasible. After initial optimization (Table S1–S4) we arrived at optimal reaction conditions furnishing O-aryl ester, 4'-benzoyloxyacetophenone (2) in 81% yield without use of an exogeneous ligand (Table 1, entry 1). First, the nature of this reaction and the nickel complexes relevant to it were explored through catalytic studies as described in the following section (Figure 2), thereafter important intermediates were investigated

through spectroscopic studies (Figure 3 and 4) in the last section.

**Catalytic studies.** To establish that exogenous ligand-free carboxylate *O*-arylation indeed operates via a self-sustained Ni<sup>I</sup>/Ni<sup>III</sup> catalytic cycle, dependency on photons was excluded (Table 1, entry 2). In addition, the rate of product formation was found to be dependent on the stirring speed, indicative for a reduction step by zinc as heterogeneous reducing agent (Figure 2A).<sup>[25]</sup> This is further supported by the tendency for this system to form nanoparticles due to over reduction of nickel at low concentrations of aryl halide (Figure S1).<sup>[24]</sup> Similar to (dtbbpy)NiBr<sub>2</sub>-catalyzed reactions a strong rate dependency on

the electronic parameter of the aryl bromides (Hammett Plot, Figure 2B) was observed.<sup>[17]</sup> Interestingly, increasing the equivalents of BzOH and <sup>t</sup>BuNH<sup>i</sup>Pr only gave a slight increase in the yield for **2** to 89% (Table 1, entry 3), in fair contrast to (dtbbpy)NiBr<sub>2</sub>-catalyzed reactions which require non-equimolar ratios of carboxylic acid, base and aryl halide.<sup>[4,5,7,8,10,26–28]</sup> Addition of dtbbpy-ligand under optimized conditions showed a declined yield of ester **2** and an increased yield in acetophenone (**3**) as byproduct (Table 1, entry 4). Therefore, based on the presented catalytic study it is proposed that the addition of dtbbpy-ligand keeps the complex in a high valent Ni(III) state for longer, promoting formation of protodehalo-

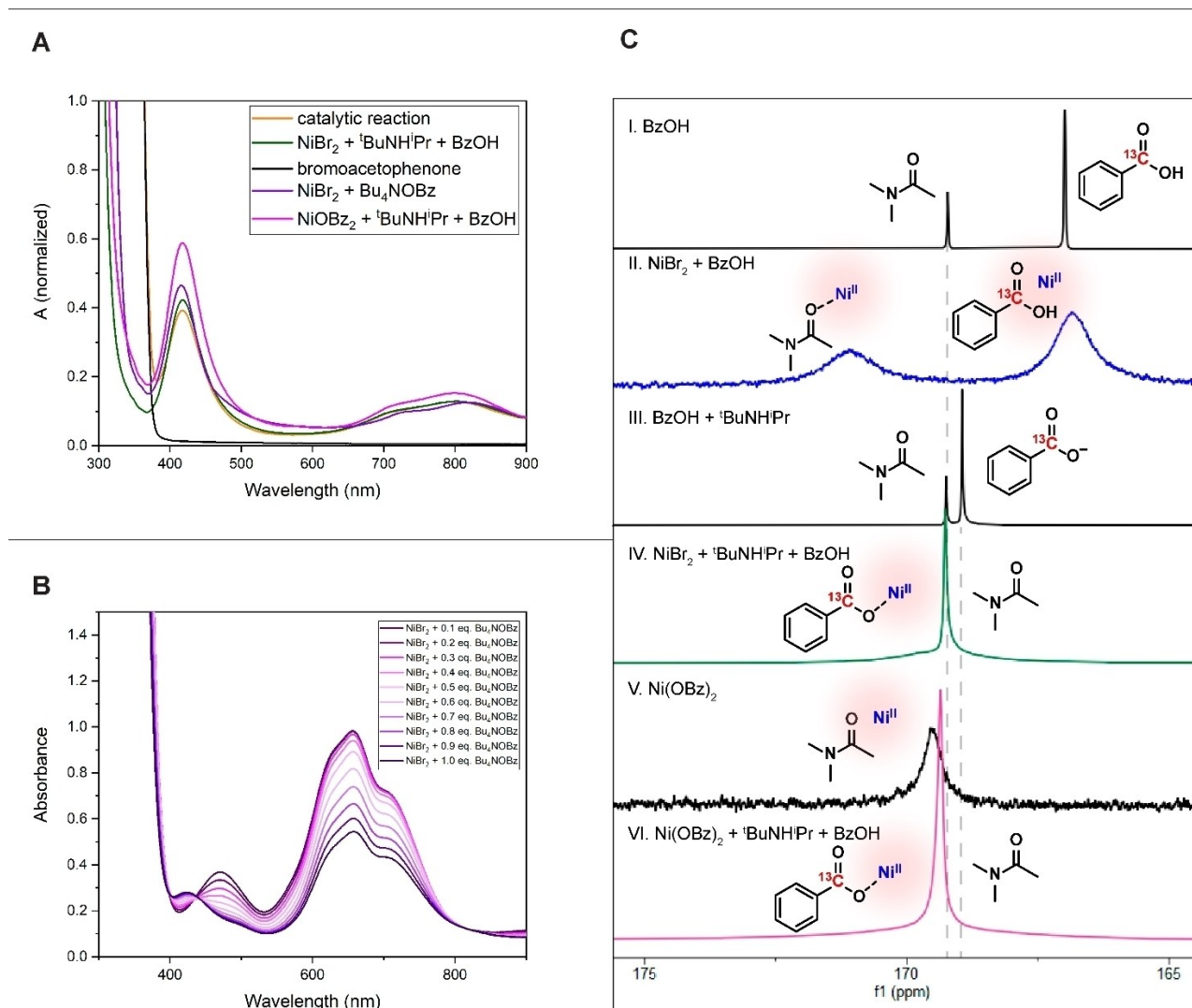
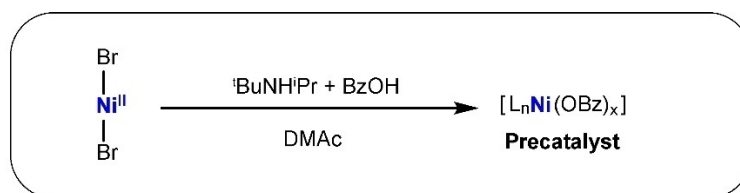
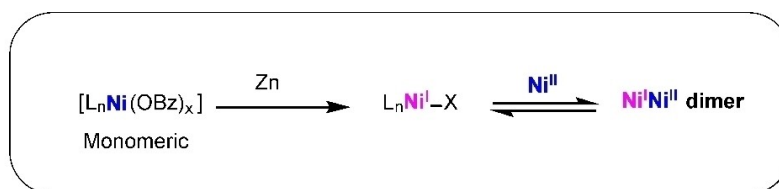
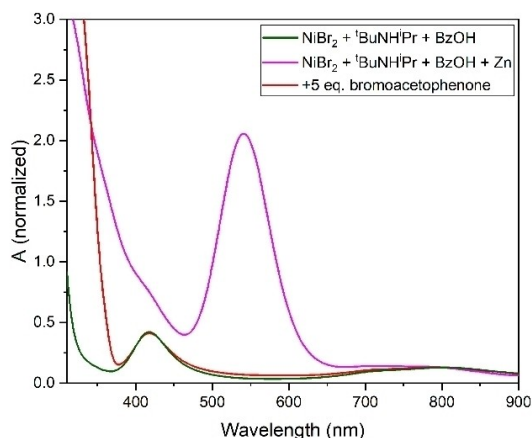


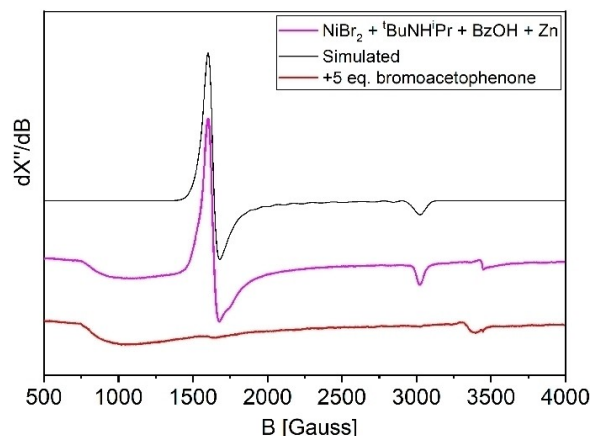
**Figure 3.** Spectroscopic investigations on the nickel system. [A] UV-Vis spectra in DMAc, catalytic reaction after 2 h (at 9% yield of **2**). [B] UV-Vis titration of a DMAc solution containing NiBr<sub>2</sub> with Bu<sub>4</sub>NOBz. [C] <sup>13</sup>C NMR spectra in DMAc.



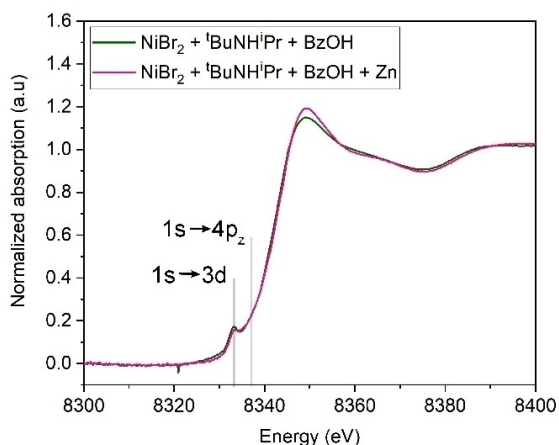
A



B



C



D

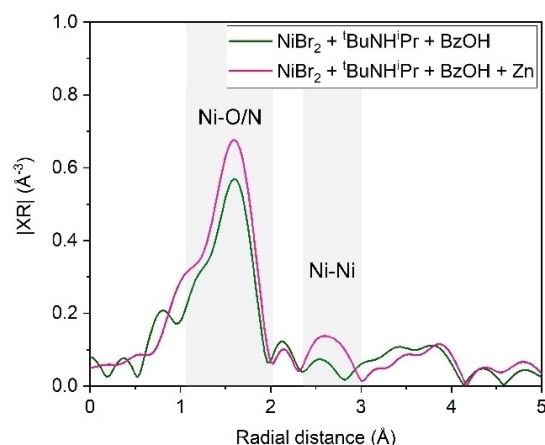


**Figure 4.** Spectroscopic investigations on the reduction of the nickel system. [A] UV-Vis spectra in DMAC. [B] X-Band EPR spectra at 10 K. [C] Ni K-edge XANES spectra of frozen DMAC solutions [D] Ni K-edge  $k^2$ -weighted Fourier transform EXAFS spectra of frozen DMAC solutions.

generated side product **3**. Nickel catalyzed carboxylate *O*-arylation using dtbbpy as ligand operates at mild temperatures (25–40 °C), but for the exogenous ligand-free reaction lowering the temperature to 40 °C had a detrimental effect on the formation of ester **2** (Table 1, entry 5), due to the slower oxidative addition at a less electron-rich nickel center. Further attempts to enable equimolar substrate ratios using the (dtbbpy)NiBr<sub>2</sub> system by changing the ligand (Table S5) or conditions (Table S8) were unproductive and lead us to pursue investigation of the exogenous ligand-free system. To gain structural insight into the complexes relevant to catalysis, the precursor was changed

for nickel(II) benzoate (Ni(OBz)<sub>2</sub>), resulting in a comparable yield for ester **2** (Table 1, entry 6), indicating that at least for the initial reduction and oxidative addition a bromide ligand is not essential. Interestingly, when DMAC (*N,N*-dimethylacetamide) as solvent is exchanged for DMF (*N,N*-dimethylformamide), greatly diminished yields are obtained (Table 1, entry 7). This can be attributed to the greatly enhanced rate of ligand exchange on DMAC complexes, the rate of ligand exchange on [Ni(DMAC)<sub>6</sub>]<sup>2+</sup> is 10<sup>3</sup> faster than on [Ni(DMF)<sub>6</sub>]<sup>2+</sup>.<sup>[29]</sup> Furthermore, whilst NiX<sub>2</sub> salts in DMF selectively form [Ni(DMF)<sub>6</sub>]<sup>2+</sup>, in DMAC five-coordinate complexes [NiX(DMAC)<sub>4</sub>]<sup>+</sup> and [NiX<sub>2</sub>(DMAC)<sub>3</sub>] exist in

solution.<sup>[30,31]</sup> We believe this to be important reasons why exogenous ligand-free nickel cross-coupling reactions are generally performed in DMAc<sup>[10][24], [23]</sup> whilst dtbbpy systems perform well in both solvents. Furthermore, as ketones are known to act as supporting ligand in similar nickel cross couplings, the reaction was performed with addition of 5 equivalents of acetophenone (Table S7, entry 11).<sup>[32,33]</sup> This had a negligible effect with ester product **2** obtained in 78% yield. Therefore, the substrate (ketone functionality) itself is not considered an essential ligand for productive catalysis.

The pivotal role of an aliphatic alkylamine base, <sup>t</sup>BuNH<sup>i</sup>Pr or NEt<sub>3</sub>, in catalysis was demonstrated by the use of other nitrogen-containing bases, which all provide inferior results with yields under 10% (Table S2, entries 5–7). Likewise, the use of tetrabutylammonium benzoate (Bu<sub>4</sub>NOBz), rather than <sup>t</sup>-BuNH<sup>i</sup>Pr and benzoic acid, gave only 7% yield for ester **2** (Table 1, entry 8). This result varies from (dtbbpy)NiBr<sub>2</sub>-catalyzed reaction, with zinc as reducing agent, which does tolerate this substrate.<sup>[10]</sup> Yet, performing catalysis with <sup>t</sup>BuNH<sub>2</sub><sup>i</sup>PrOBz gave ester product **2** with a yield of 78% (Table S2, entry 3). These findings clearly indicate a more elaborate role for <sup>t</sup>BuNH<sup>i</sup>Pr, even when protonated, than solely functioning as a Brønsted base. Summarizing the catalytic experiments, we propose that in absence of the dtbbpy-ligand, protodehalogenation and deleterious comproportionation reactions are prevented. This enables the formation of *O*-aryl esters from equimolar amounts of coupling partners. In contrast, for the (dtbbpy)NiBr<sub>2</sub>-catalyzed reaction an excess of carboxylate substrate is required to prevent unproductive comproportionation of Ni<sup>i</sup> and Ni<sup>iii</sup>.<sup>[10]</sup> However, for this reaction the electron-donating effect of the dtbbpy-ligand could have a positive effect on the rate of oxidative addition, and hence catalysis can be performed at a lower reaction temperature (Table S8). Therefore, the exogenous ligand-free system shows diminished activity at 40 °C (Table 1, entry 2) whereas the (dtbbpy)NiBr<sub>2</sub>-catalyzed reaction is less effective at elevated temperatures.

**Spectroscopic investigation.** To elucidate the nature of the Ni<sup>ii</sup> precatalyst and catalytic intermediates under exogenous ligand-free conditions we performed spectroscopic studies. UV-Vis spectra of the catalytic reaction mixture (Figure 3A, orange trace) and a DMAc solution containing NiBr<sub>2</sub>, <sup>t</sup>BuNH<sup>i</sup>Pr and BzOH (Figure 3A, green trace) proved to be identical, disclosing a Ni<sup>ii</sup> resting state. Additionally, DMAc solutions containing Ni(OBz)<sub>2</sub>, <sup>t</sup>BuNH<sup>i</sup>Pr and BzOH (Figure 3A, pink trace) or NiBr<sub>2</sub> and tetrabutylammonium benzoate (Bu<sub>4</sub>NOBz) (Figure 3A, purple trace) gave fairly similar UV-Vis spectra. Indicating that bromide and the amine base do not coordinate to the bulk of nickel. The exchange of the bromide ligand for benzoate anions was further demonstrated in a UV-Vis titration of a DMAc solution containing NiBr<sub>2</sub> with up to 20 eq. of Bu<sub>4</sub>NOBz (Figure 3B and Figure S9). The addition of 0.1 to 1 eq. Bu<sub>4</sub>NOBz provides an isobestic point at 436 nm and a decrease in the bands at 470 nm, 630, 660 nm and the shoulder at 700 nm. These bands were assigned by Ishiguro and co-workers to be [NiBr(DMAC)<sub>4</sub>]<sup>+</sup> (460 nm), NiBr<sub>2</sub>(DMAC)<sub>2</sub> (600 nm) and [NiBr<sub>3</sub>(DMAC)]<sup>-</sup> (660 nm with a shoulder 700 nm).<sup>[31]</sup> That the amine base primarily exists in the protonated, and the benzoic acid in the deprotonated

form was further demonstrated via <sup>1</sup>H and <sup>13</sup>C NMR studies using <sup>13</sup>C-labeled benzoic acid (Figure S12, S13 and Figure 3C).<sup>[34]</sup> Comparison of the chemical shifts of BzOH- $\alpha$ -<sup>13</sup>C (167 ppm), BzO<sup>-</sup>- $\alpha$ -<sup>13</sup>C (169 ppm) and mixtures of NiBr<sub>2</sub> or Ni(OBz)<sub>2</sub> with <sup>t</sup>BuNH<sup>i</sup>Pr and BzOH in DMAc reveal that during catalysis the nucleophile is present as benzoate (Figure 3C; I, III, IV and VI). The line broadening and downfield shift of the benzoate signals can be explained by exchange between free and coordinated benzoate (Figure 3C; IV and VI). While coordination of DMAc was observed for NiBr<sub>2</sub> (~171 ppm) and BzOH- $\alpha$ -<sup>13</sup>C in DMAc (Figure 3C; II). For mixtures of NiBr<sub>2</sub> or Ni(OBz)<sub>2</sub> including <sup>t</sup>BuNH<sup>i</sup>Pr and BzOH (Figure 3C; IV and VI) no or minimal exchange of DMAc (on NMR timescale) is present. For further structural characterization we turned to X-ray absorption spectroscopy (XAS), since Ni K-edge XAS has shown to be a valuable spectroscopic tool for the elucidation of the local structure including geometry of molecular coordination complexes as well as their electronic structures.<sup>[35–37]</sup> For a DMAc solution containing NiBr<sub>2</sub>, <sup>t</sup>BuNH<sup>i</sup>Pr and BzOH the X-ray absorption near edge structure spectrum (XANES) (Figure 4C, green trace) reveals a distinct pre-edge peak at 8333 eV which can be assigned to a 1s→3d electronic transition, while the 1s→4p<sub>z</sub> electronic transition (expected at 8337 eV) is absent thereby excluding the formation of complexes lacking one or more axial ligands (square planar and square pyramidal geometries).<sup>[38]</sup>

More structural parameters were determined by Extended X-ray absorption fine structure (EXAFS) analysis, with figure 4D providing the Fourier Transform (FT) EXAFS function. The absence of any remote nickel shell, as observed for a DMAc solution containing only NiBr<sub>2</sub> and <sup>t</sup>BuNH<sup>i</sup>Pr (Figure S19), is indicative for monomeric nickel complexes present in solution with 2.65(18) Ni–O/Ni–N at 2.068(1) Å (Figure 4D, green trace, for details see S.I.). However, solely based on nickel K-edge EXAFS data an exact coordination number of the bromide shell cannot be determined reliably due to the almost complete anti-phase behavior of different Ni–Br contributions, when present at slightly different distances (Figure S20–S22).<sup>[39]</sup> This means that these EXAFS data suggest that either no Ni–Br contributions are present, or that an even number of Ni–Br contributions (at different distances) are present. In order to provide more detail hereon, follow-up studies could include additional bromine K-edge XAS measurements, which would also possibly give information on whether zinc is acting as a bromide sponge during catalysis.<sup>[37,40]</sup> To summarize, <sup>t</sup>BuNH<sup>i</sup>Pr was found to be essential in catalytic experiments, while our spectroscopic investigations indicate that the Brønsted base primarily exists in the protonated form (<sup>t</sup>BuNH<sub>2</sub><sup>i</sup>Pr<sup>+</sup>). Moreover, because of the identical catalytic activity of NiBr<sub>2</sub> and Ni(OBz)<sub>2</sub> as well as the spectroscopic similarity (UV-Vis and <sup>13</sup>C NMR) we propose that the bulk of the nickel that forms the precatalyst is present as a mixture of monomeric complexes of the type [L<sub>n</sub>Ni(OBz)<sub>x</sub>].

More insight into the reduction of the formed Ni<sup>ii</sup> species was obtained by stirring a Ni<sup>ii</sup>-precursor solution (a DMAc solution containing NiBr<sub>2</sub>, <sup>t</sup>BuNH<sup>i</sup>Pr and BzOH) in the presence of excess zinc.<sup>[41]</sup> The *in situ* reduced Ni<sup>ii</sup>-precursor solution was studied by UV-Vis, EPR and XAS spectroscopy. In the UV-Vis

spectrum a new band at 541 nm is observed, as well as a shoulder at ~415 nm originating from non-reduced Ni<sup>II</sup> (Figure 4A, pink trace). EPR spectroscopy on this solution provided a spectrum with a characteristic  $S=3/2$  signal (Figure 4B, pink trace, for simulation details see Figure S14). Based on Ni K-edge XANES data the formation of complexes deprived of axial ligands (square pyramidal or square planar geometries) can be excluded (Figure 4C, pink trace). EXAFS analysis indicates an increase in the Ni–O/Ni–N shell (3.1(3)) at a bond distance of 2.04(1) Å and, more importantly, the emergence of a Ni–Ni shell at 3.10(3) Å with a coordination number of 0.6(5) (Figure 4D, pink trace, for details see SI). Overall, it can be rationalized that Ni<sup>II</sup> is reduced by zinc to Ni<sup>I</sup> which subsequently forms a bimetallic nickel intermediate in the absence of aryl halide. The trapping of formed Ni<sup>I</sup> by excess Ni<sup>II</sup> in solution leading to an off-cycle Ni<sup>I</sup>–Ni<sup>II</sup> dimer was also reported by Nocera and co-workers in the nickel-catalyzed aryl etherification by (dtbbpy)NiCl<sub>2</sub> in the presence of quinuclidine and a photocatalyst or zinc.<sup>[14]</sup> Dimeric nickel complexes have been identified before as important intermediates in nickel-catalyzed cross-coupling, but this represents the first observation of a Ni<sup>I</sup>–Ni<sup>II</sup> dimer under exogenous ligand-free conditions.<sup>[14,20,21]</sup>

Next, the reactivity of the *in situ* formed Ni<sup>I</sup>–Ni<sup>II</sup> dimer was examined. Therefore we treated the pink-colored nickel solution, obtained after reduction, with 5 equiv. of 4'-bromoacetophenone and heated to 70 °C which resulted in a yellow-colored reaction mixture after 30 min (no color change was observed at R.T.). UV-Vis and EPR spectroscopy revealed the complete disappearance of the UV-Vis band at 541 nm (Figure 4A, red trace) and the  $S=3/2$  signal in the EPR spectrum (Figure 4B, red trace). The relevance of the Ni<sup>I</sup>–Ni<sup>II</sup> dimer as an off-cycle species was further evaluated in an experiment, where NiBr<sub>2</sub> in the presence of <sup>t</sup>BuNH<sup>i</sup>Pr and BzOH, was first reduced with zinc for 3 hours (see Figure S11 for UV-Vis spectrum). Next, this solution was filtered, to remove zinc, and 20 equiv. of bromoacetophenone were supplied and the mixture was stirred at 70 °C for 30 min. Subsequent GC analysis revealed minor formation of *O*-aryl ester **2** (yield <2%). Diminishing the reduction time to 30 min. (see Figure S11 for UV-Vis spectrum), resulted in no ester product **2** formation. These results are notable since it contrasts with other studies into nickel-catalyzed C-heteroatom bond formations, where: 1) dimeric nickel complexes proved to be unreactive towards aryl halides<sup>[19,20]</sup> or 2) high concentrations of low-valent nickel had a detrimental effect due to the facile formation of inactive states such as nickel black, Ni<sup>II</sup> or Ni<sup>I</sup>–Ni<sup>I</sup> dimers.<sup>[14,24]</sup>

To demonstrate the applicability of the developed protocol for exogenous ligand-free nickel-catalyzed ester bond formation with equimolar amounts of aryl halide, carboxylic acid and base we examined the scope of this reaction (Figure 5). Changing the aryl bromide from **1** (81%) to 4'-iodoacetophenone **5** gave the corresponding ester product **2** in a good yield (87%). Even when using aryl chloride **6**, catalytic product formation was observed albeit with lowered yields (21%). Aryl halides lacking sufficient electron-withdrawing groups show low reactivity (**8**, **9**, **10**) presumably because of a slow rate for oxidative addition. A variety of electron-poor aryl bromides were found to be

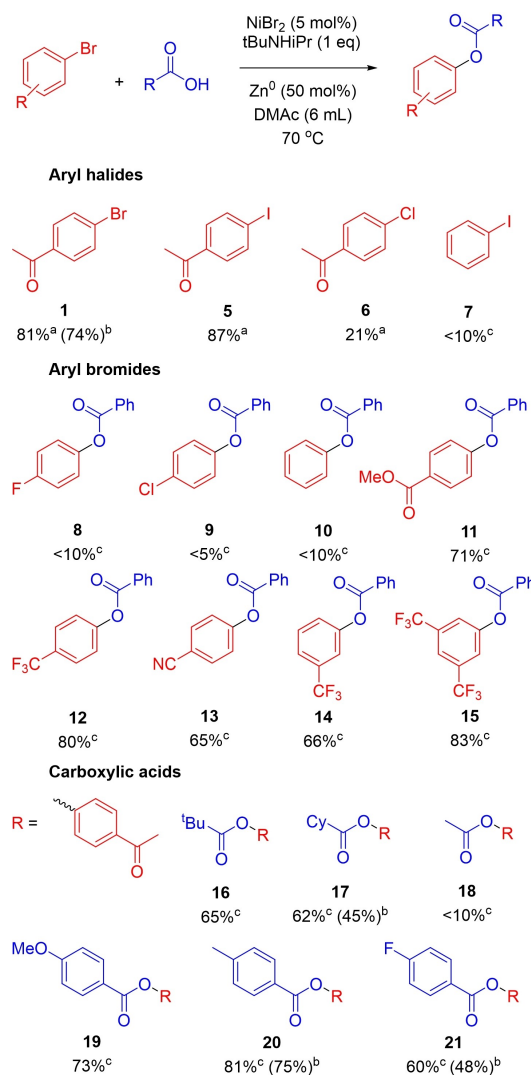


**Figure 5.** Substrate scope of NiBr<sub>2</sub>-catalyzed esterification of carboxylic acids and aryl bromides. [a] Yield determined by GC with mesitylene as internal standard after 20 hours reaction time. [b] Isolated yield. [c] Yield determined by <sup>1</sup>H NMR with 1,3,5-Tri-tert-butylbenzene as internal standard after 24 hours reaction time.

effective coupling partners (**11–15**). For the carboxylic acid coupling partner, sterically hindered pivalic acid and cyclohexanecarboxylic acid (**16**, **17**) furnished the corresponding ester efficiently, as well as various aromatic carboxylic acids (**19–21**). Only acetic acid hampered catalysis and afforded the ester product (**18**) in poor yield (<10%).

To provide an opening for future studies into photocatalyzed nickel carboxylate *O*-arylation, we investigated the herein developed exogenous ligand-free system under photocatalytic conditions. Zinc was replaced by the competent photocatalyst (Ir(ppy)<sub>3</sub>) which only furnished ester product **2** in moderate yields, also for a reaction with excess BzOH and <sup>t</sup>BuNH<sup>i</sup>Pr (Table S6, entries 1 and 2) which is in contrast to the (dtbbpy)NiBr<sub>2</sub>-catalyzed reaction (Table S6, entry 3).<sup>[4]</sup> Previous studies showed that in ligand-based systems, (dtbbpy)NiBr<sub>2</sub> directly quenches the excited photocatalyst and that <sup>t</sup>BuNH<sup>i</sup>Pr



has no function in the photocatalysis.<sup>[42,43]</sup> Moreover, in ligand-free C–N cross-coupling 1,4-diazabicyclo[2.2.2]octane (DABCO) is employed as a base and serves also as a quenching agent for the excited Ir<sup>III\*</sup> photocatalyst, being oxidized to generate Ir<sup>IV</sup> which consecutively reduces Ni<sup>II</sup>.<sup>[17]</sup> However, for ligand-free carboxylate *O*-arylation the addition of DABCO diminished the formation of ester **2** (Table S6, entry 4).

The incompatibility of DABCO with ligand-free conditions was also displayed in a reaction with zinc as reducing agent, which resulted in no formation of ester **2** (Table S6, entry 5). This is presumably caused by coordination of DABCO inhibiting catalysis, similar to inhibition we observed by addition of COD as poison (Table S7, entry 6). Furthermore, photoinitiation with visible light (405 nm) afforded ester **2** only in moderate yields (Table S6, entries 6 and 7). These results show that it could be possible to enable equimolar photocatalytic exogenous ligand-free nickel-catalyzed carboxylate *O*-arylation, if a compatible quencher which preferably also serves as the base is found.

## Summary and Conclusion

In summary, the here presented mechanistic studies of nickel-catalyzed carboxylate *O*-arylation have uncovered the competition between productive catalysis and off-cycle pathways (comproportionation and protodehalogenation) that exists for all fundamental elementary steps. In the absence of an exogenous dtbbpy-ligand these deleterious reactions were significantly suppressed allowing equimolar amounts of coupling partners. The spectroscopic investigation of this novel catalytic system revealed that during catalysis the bulk of Ni<sup>II</sup> is present in the form of [L<sub>n</sub>Ni(OBz)<sub>2</sub>]<sub>n</sub>, yet for catalysis an alkylamine base was essential. Studies into the reduction of the Ni<sup>II</sup>-precursor identified a bimetallic pathway resulting in an off-cycle Ni<sup>I</sup>–Ni<sup>II</sup> dimer. The presented insights into the reaction pathways of the commonly proposed self-sustained Ni<sup>I</sup>/Ni<sup>II</sup> catalytic cycle reveal that for carboxylate *O*-arylation a choice must be made between either mild conditions or equimolar ratios of substrates. Thereby, we believe this knowledge will be relevant for the design of novel efficient nickel-catalyzed C–heteroatom bond formations under mild conditions.

## Experimental Section

### General Experimental Details

Chemicals were obtained from Fluorochem or Merck and used without further purification, unless noted otherwise. Anhydrous *N,N*-Dimethylacetamide 99% (abbreviated DMAc) was degassed by bubbling argon through for > 60 min, and dried over 4 Å molecular sieves. All air-sensitive materials were manipulated using standard Schlenk techniques (under argon) or by the use of a nitrogen-filled glovebox (MBraun Unilab). Ni(OBz)<sub>2</sub>·3H<sub>2</sub>O and Ni(OBz- $\alpha$ -<sup>13</sup>C)<sub>2</sub>·3H<sub>2</sub>O (abbreviated NiOBz<sub>2</sub>) were synthesized and zinc was activated following literature procedures.<sup>[44,45]</sup> NiBr<sub>2</sub>·2-methoxyethylether (abbreviated NiBr<sub>2</sub>), tetrabutylammoniumbenzoate (Bu<sub>4</sub>NOBz) and activated zinc were stored and weighed in a nitrogen-filled glovebox. The NMR solvent C<sub>6</sub>D<sub>6</sub> was dried over molecular sieves and

degassed via three freeze-pump-thaw cycles. <sup>1</sup>H (500 or 400 MHz), <sup>13</sup>C (125 or 100 MHz) and <sup>19</sup>F NMR (376 MHz) spectra were recorded on a Bruker DRX 500 MHz or a Bruker AVANCE 400 MHz spectrometer and referenced against residual solvent signal. The NMR yields were determined by integrating the signals of the product against the tert-butyl protons of 1,3,5-Tri-tert-butylbenzene (internal standard), as shown in the crude NMR spectra. UV-Vis spectra were collected on a double beam Shimadzu UV-2600 spectrometer in a 1.0 cm quartz cuvette with DMAc as reference. GC analysis was performed on a Thermo Scientific Trace GC Ultra equipped with a Rxi-5 ms fused silica column (30.0 m×0.25 mm×0.25 μm). Temperature program: initial temperature 50 °C, heat to 200 °C with 8.0 °C min<sup>-1</sup>, heat to 250 °C with 50 °C min<sup>-1</sup>, hold for 6 minutes. Inlet temperature 250 °C, split ratio of 30, 1.0 mL min<sup>-1</sup> helium flow, FID temperature 250 °C. For GC measurements mesitylene was used as internal standard and GC calibration curves were composed for 4'-bromoacetophenone (**1**), acetophenone (**3**), 4'-benzoyloxyacetophenone (**2**) and 4'-hydroxyacetophenone (**4**) (Figure S32). GC-HRMS (HRMS) measurements were performed on a Jeol AccuTOF GC v 4 g, JMS-T100GCV Mass spectrometer equipped with a field desorption (FD) / field ionization (FI) probe, fitted with a 10 μm tungsten FI emitter. Samples were diluted with acetone and mesitylene was used as an internal calibrant. Here, GC analysis was conducted on a Thermo Scientific Trace GC Ultra equipped with an Agilent 19091S-433 column (30.0 m×0.25 mm×0.25 μm). Temperature program: initial temperature 50 °C, heat to 315 °C with 15 °C min<sup>-1</sup>, hold for 5 min. Inlet temperature 230 °C, split ratio of 15:1, 1.0 mL min<sup>-1</sup> helium flow and GC interface at 250 °C. For the field ionization (FI) a flashing current of 40 mA on every spectrum of 30 ms was applied. EPR measurements were performed in airtight J.Young quartz tubes in an atmosphere of purified argon. Frozen solution EPR spectra were recorded on a Bruker EMX-plus CW X-band spectrometer equipped with a Bruker ER 4112HV-CF100 helium cryostat. The spectra were obtained on freshly prepared solutions of nickel compounds and simulated using EasySpin<sup>[46]</sup> via the cwEPR GUI.<sup>[47]</sup>

### General experiment for catalysis

In a nitrogen-filled glovebox, NiBr<sub>2</sub> (21.2 mg, 0.06 mmol) and zinc (39.2 mg, 0.6 mmol) were weighed and transferred to a Schlenk flask (20 mL). The flask was removed from the glovebox, the atmosphere changed to argon, and the solids 4-bromoacetophenone (239 mg, 1.2 mmol) and benzoic acid (147 mg, 1.2 mmol) were added. Directly thereafter, DMAc (6 mL) and <sup>t</sup>BuNH<sup>i</sup>Pr (190 μL, 1.2 mmol) were supplied via a syringe and the temperature was increased to 70 °C with stirring at 1400 rpm. After 20 h reaction time, 60 μL mesitylene (internal standard) was added and approximately 10 μL of the reaction mixture was diluted with 2 mL acetone, filtered over a 45 μm syringe filter and analyzed with GC.

## Acknowledgements

*This work is part of the Advanced Research Center for Chemical Building Blocks, ARC CBBC, which is co-founded and co-financed by the Netherlands Organization for Scientific Research (NWO, contract 736.000.000) and the Netherlands Ministry of Economic Affairs and Climate.*

## Conflict of Interest

The authors declare no conflict of interest.

## Data Availability Statement

The data that support the findings of this study are available from the corresponding author upon reasonable request.

**Keywords:** Nickel catalysis · C-heteroatom bond formations · carboxylate O-arylation · Esterification

- [1] O. S. Wenger, *Chem. Eur. J.* **2021**, *27*, 2270–2278.
- [2] C. Zhu, H. Yue, J. Jia, M. Rueping, *Angew. Chem. Int. Ed.* **2021**, *60*, 17810–17831.
- [3] J. B. Dicciani, T. Diao, *Trend Chem.* **2019**, 1–15.
- [4] E. R. Welin, C. Le, D. M. Arias-Rotondo, J. K. McCusker, D. W. C. MacMillan, *Science*. **2017**, *355*, 380–385.
- [5] M. He, S. Yang, X. Yu, M. Bao, *Synlett* **2021**, 32, A–E.
- [6] D. L. Zhu, H. X. Li, Z. M. Xu, H. Y. Li, D. J. Young, J. P. Lang, *Org. Chem. Front.* **2019**, *6*, 2353–2359.
- [7] B. Pieber, J. A. Malik, C. Cavedon, S. Gisbertz, A. Savateev, D. Cruz, T. Heil, G. Zhang, P. H. Seeberger, *Angew. Chem. Int. Ed.* **2019**, *58*, 9575–9580; *Angew. Chem.* **2019**, *131*, 9676–9681.
- [8] J. Lu, B. Pattengale, Q. Liu, S. Yang, W. Shi, S. Li, J. Huang, J. Zhang, *J. Am. Chem. Soc.* **2018**, *140*, 13719–13725.
- [9] Y. Mo, Z. Lu, G. Rughoobur, P. Patil, N. Gershenfeld, A. I. Akinwande, S. L. Buchwald, K. F. Jensen, *Science*. **2020**, *368*, 1352–1357.
- [10] R. Sun, Y. Qin, D. G. Nocera, *Angew. Chem. Int. Ed.* **2020**, *59*, 9527–9533; *Angew. Chem.* **2020**, *132*, 9614–9620.
- [11] H. Kitano, H. Ito, K. Itami, *Org. Lett.* **2018**, *20*, 2428–2432.
- [12] L. Li, F. Song, X. Zhong, Y. D. Wu, X. Zhang, J. Chen, Y. Huang, *Adv. Synth. Catal.* **2020**, *362*, 126–132.
- [13] B. J. Shields, B. Kudisch, G. D. Scholes, A. G. Doyle, *J. Am. Chem. Soc.* **2018**, *140*, 3035–3039.
- [14] R. Sun, Y. Qin, S. Ruccolo, C. Schnedermann, C. Costentin, D. G. Nocera, *J. Am. Chem. Soc.* **2019**, *141*, 89–93.
- [15] Y. Qin, R. Sun, N. P. Gianoulis, D. G. Nocera, *J. Am. Chem. Soc.* **2021**, *143*, 2005–2015.
- [16] L. Yang, H. H. Lu, C. H. Lai, G. Li, W. Zhang, R. Cao, F. Liu, C. Wang, J. Xiao, D. Xue, *Angew. Chem. Int. Ed.* **2020**, *59*, 12714–12719; *Angew. Chem.* **2020**, *132*, 12814–12819.
- [17] N. A. Till, L. Tian, Z. Dong, G. D. Scholes, D. W. C. MacMillan, *J. Am. Chem. Soc.* **2020**, *142*, 15830–15841.
- [18] Y. Kawamata, J. C. Vantourout, D. P. Hickey, P. Bai, L. Chen, Q. Hou, W. Qiao, K. Barman, M. A. Edwards, A. F. Garrido-Castro, J. N. deGruyter, H. Nakamura, K. Knouse, C. Qin, K. J. Clay, D. Bao, C. Li, J. T. Starr, C. Garcia-Irizarry, N. Sach, H. S. White, M. Neurock, S. D. Minter, P. S. Baran, *J. Am. Chem. Soc.* **2019**, *141*, 6392–6402.
- [19] N. A. Till, S. Oh, D. W. C. MacMillan, M. J. Bird, *J. Am. Chem. Soc.* **2021**, *143*, 9332–9337.
- [20] M. Mohadjer Beromi, G. W. Brudvig, N. Hazari, H. M. C. Lant, B. Q. Mercado, *Angew. Chem. Int. Ed.* **2019**, *58*, 6094–6098; *Angew. Chem.* **2019**, *131*, 6155–6159.
- [21] S. I. Ting, W. L. Williams, A. G. Doyle, *J. Am. Chem. Soc.* **2022**, DOI 10.26434/chemrxiv-2022-m8xj2.
- [22] H. Na, L. M. Mirica, *Nat. Commun.* **2022**, *13*, 1–11.
- [23] E. B. Corcoran, M. T. Pimot, S. Lin, S. D. Dreher, D. A. Dirocco, I. W. Davies, S. L. Buchwald, D. W. C. Macmillan, *Science*. **2016**, *353*, 279–283.
- [24] S. Gisbertz, S. Reischauer, B. Pieber, *Nat. Catal.* **2020**, *3*, 611–620.
- [25] D. Han, S. Li, S. Xia, M. Su, J. Jin, *Chem. Eur. J.* **2020**, *26*, 12349–12354.
- [26] D. L. Zhu, H. X. Li, Z. M. Xu, H. Y. Li, D. J. Young, J. P. Lang, *Org. Chem. Front.* **2019**, *6*, 2353–2359.
- [27] E. O. Bortnikov, S. N. Semenov, *J. Org. Chem.* **2021**, *86*, 782–793.
- [28] W. Zu, C. Day, L. Wei, X. Jia, L. Xu, *Chem. Commun.* **2020**, *56*, 8273–8276.
- [29] S. F. Lincoln, A. M. Hounslow, A. N. Boffa, *Inorg. Chem.* **1986**, *25*, 1038–1041.
- [30] H. Suzuki, S. Ishiguro, *Inorg. Chem.* **1992**, *31*, 4178–4183.
- [31] M. Koide, H. Suzuki, S. Ichi Ishiguro, *J. Solution Chem.* **1994**, *23*, 1257–1270.
- [32] A. K. Cooper, D. K. Leonard, S. Bajo, P. M. Burton, D. J. Nelson, *Chem. Sci.* **2020**, *11*, 1905–1911.
- [33] A. N. Desnoyer, W. He, S. Behyan, W. Chiu, J. A. Love, P. Kennepohl, *Chem. A Eur. J.* **2019**, *25*, 5259–5268.
- [34] H. Lundberg, F. Tinnis, J. Zhang, A. G. Algarra, F. Himo, H. Adolfsson, *J. Am. Chem. Soc.* **2017**, *139*, 2286–2295.
- [35] W. Hao, Y. Sha, Y. Deng, Y. Luo, L. Zeng, S. Tang, Y. Weng, C. W. Chiang, A. Lei, *Chem. Eur. J.* **2019**, *25*, 4931–4934.
- [36] J. Rabeah, J. Radnik, V. Briois, D. Maschmeyer, G. Stochniol, S. Peitz, H. Reeker, C. La Fontaine, A. Brückner, *ACS Catal.* **2016**, *6*, 8224–8228.
- [37] M. P. Feth, A. Klein, H. Bertagnolli, *Eur. J. Inorg. Chem.* **2003**, 839–852.
- [38] G. J. Colpas, M. J. Maroney, C. Bagyinka, M. Kumar, W. S. Willis, S. L. Suib, N. Baidya, P. K. Mascharak, *Inorg. Chem.* **1991**, *30*, 920–928.
- [39] M. Tromp, J. A. Van Bokhoven, A. M. Arink, J. H. Bitter, G. Van Koten, D. C. Koningsberger, *Chem. Eur. J.* **2002**, *8*, 5667–5678.
- [40] J. Evans, W. Levason, R. J. Perry, *J. Chem. Soc. Dalton Trans.* **1992**, 1497–1501.
- [41] Q. Lin, T. Diao, *J. Am. Chem. Soc.* **2019**, *141*, 17937–17948.
- [42] L. Tian, N. A. Till, B. Kudisch, D. W. C. MacMillan, G. D. Scholes, *J. Am. Chem. Soc.* **2020**, *142*, 4555–4559.
- [43] S. I. Ting, S. Garakyaraghi, C. M. Taliaferro, B. J. Shields, G. D. Scholes, F. N. Castellano, A. G. Doyle, *J. Am. Chem. Soc.* **2020**, *142*, 5800–5810.
- [44] A. Vráblová, L. R. Falvello, J. Campo, J. Miklovič, R. Boča, J. Černák, M. Tomáš, *Eur. J. Inorg. Chem.* **2016**, 928–934.
- [45] C. R. Smith, *Synlett* **2009**, 1522–1523.
- [46] S. Stoll, A. Schweiger, *J. Magn. Reson.* **2006**, *178*, 42–55.
- [47] T. Casey, “cwEPR (<https://www.mathworks.com/matlabcentral/fileexchange/73292-cwep>)”, MATLAB Central File Exchange. Retrieved December 13, 2021, 2021.

Manuscript received: April 24, 2022  
Revised manuscript received: July 11, 2022  
Accepted manuscript online: July 12, 2022  
Version of record online: August 11, 2022